

Article

Formation and Characterization of Various ZnO/SiO₂-Stacked Layers for Flexible Micro-Energy Harvesting Devices

Chongsei Yoon , Buil Jeon and Giwan Yoon *

School of Electrical Engineering, Korea Advanced Institute of Science and Technology, 291 Daehak-ro, Yuseong-gu, Daejeon 34141, Korea; csyoon16@kaist.ac.kr (C.Y.); jurn678@kaist.ac.kr (B.J.)

* Correspondence: gwyoon@kaist.ac.kr; Tel.: +82-42-350-7411

Received: 8 June 2018; Accepted: 8 July 2018; Published: 11 July 2018



Abstract: In this paper, we present a study of various ZnO/SiO₂-stacked thin film structures for flexible micro-energy harvesting devices. Two groups of micro-energy harvesting devices, SiO₂/ZnO/SiO₂ micro-energy generators (SZS-MGs) and ZnO/SiO₂/ZnO micro-energy generators (ZSZ-MGs), were fabricated by stacking both SiO₂ and ZnO thin films, and the resulting devices were characterized. With a particular interest in the fabrication of flexible devices, all the ZnO and SiO₂ thin films were deposited on indium tin oxide (ITO)-coated polyethylene naphthalate (PEN) substrates using a radio frequency (RF) magnetron sputtering technique. The effects of the thickness and/or position of the SiO₂ films on the device performance were investigated by observing the variations of output voltage in comparison with that of a control sample. As a result, compared to the ZnO single-layer device, all the ZSZ-MGs showed much better output voltages, while all the SZS-MG showed only slightly better output voltages. Among the ZSZ-MGs, the highest output voltages were obtained from the ZSZ-MGs where the SiO₂ thin films were deposited using a deposition power of 150 W. Overall, the device performance seems to depend significantly on the position as well as the thickness of the SiO₂ thin films in the ZnO/SiO₂-stacked multilayer structures, in addition to the processing conditions.

Keywords: silicon dioxide; piezoelectric device; zinc oxide; RF sputtering deposition

1. Introduction

With the recent rapid development of more advanced wireless sensors for the Internet of Things (IoT) and wearable electronic devices, the demand for devices that can harvest various forms of ambient energy, such as mechanical vibration [1], acoustic waves [2], human biomechanical movement [3], water waves [4], environmental wind [5], solar radiance [6], and even waste heat [7] has become increasingly urgent. Among the various energy harvesting technologies recently developed, piezoelectric energy harvesting technology is expected to play an important role as a potential energy source to power numerous sensors and devices in the near future. Piezoelectric technology converts mechanical energy into electrical energy by exploiting the piezoelectric effect in certain materials. Zinc oxide (ZnO) is a piezoelectric material frequently used for the fabrication of energy harvesting devices due to its large piezoelectric constant and superior film quality [8]. It is also environmentally friendly and biocompatible because it contains no toxic elements such as lead. In general, lead-free ZnO-based piezoelectric materials are available for wearable piezoelectric devices. Moreover, the lead-free materials are particularly advantageous in transducers for the underwater and medical imaging applications mainly due to their relatively low density as well as lower acoustical impedance [9,10].

Many research teams worldwide have tried to develop ZnO-based energy harvesting devices while making an effort to maximize their piezoelectric performance. Prof. Z. L. Wang and his team

from Georgia Institute of Technology proposed a method of fabricating vertically integrated structures to serve as nanogenerators using piezoelectric ZnO nanowires, polymethyl methacrylate (PMMA), and Au electrodes [11]. The vertically integrated structures can be fabricated using conventional complementary metal-oxide-semiconductor (CMOS) process technology. They are also more durable than other device structures such as laterally integrated or radially integrated nanogenerators [12,13]. Their fabrication seems to be cost-effective because all that is required to fabricate these micro-energy generators is simply the stacking of thin film layers. Similarly, high-efficiency piezoelectric ZnO-based nanogenerators have also been developed for energy harvesting applications by forming ZnO/AlN-stacked layers [14] and adopting free-carrier-modulated ZnO:N piezoelectric thin films [15]. Moreover, there have been attempts to improve the piezoelectric materials or the device performance by adopting new electrodes or forming a p-n junction to block the screening effect based on energy band considerations [15–18]. The screening effect means that the piezoelectric potential (piezopotential) induced through the piezoelectric ZnO film is canceled by free electrons that exist inherently in a semiconductive ZnO material or electrode. This reduces the net potential across the ZnO film, thus degrading device performance. Therefore, to maximize the device output performance, it is essential to suppress the screening effect more effectively by controlling the ZnO free carrier density [15]. Some research teams have used insulators or other semiconductor materials to form a good potential barrier to increase output voltages [19]. Other research using AlN or various oxides (MoO_x, Cu₂O, and NiO) has been reported [14,16,18,20]. Despite such intensive research, only few studies were published using SiO₂ as an insulator [21]. SiO₂, an excellent insulating material, is electrically reliable, biocompatible, non-toxic, cheap, and easy to fabricate. Therefore, it seems highly desirable to adopt SiO₂ as an insulating interlayer in ZnO-based piezoelectric devices.

In this paper, we present a study of various ZnO/SiO₂-stacked thin film structures for flexible micro-energy harvesting devices. Two different groups of micro-energy harvesting devices, i.e., SiO₂/ZnO/SiO₂ micro-energy generators (SZS-MGs) and ZnO/SiO₂/ZnO micro-energy generators (ZSZ-MGs), were fabricated by stacking both SiO₂ and ZnO thin films on top of each other, and subsequently characterized. With a particular interest in the fabrication of flexible devices, all the ZnO and SiO₂ thin films were deposited on flexible indium tin oxide (ITO)-coated polyethylene naphthalate (PEN) substrates using a radio frequency (RF) magnetron sputtering technique. The effects of the thickness and position of the deposited SiO₂ films on the device performance were investigated by observing the variations in the output voltages in comparison with the ZnO single-layer device used as a control sample. As a result, compared to the ZnO single-layer device, all the ZSZ-MGs showed much better output voltages, while all the SZS-MGs showed slightly better output voltages. Among the ZSZ-MGs, the highest output voltages were obtained from the ZSZ-MG with the SiO₂ thin films deposited at a deposition power of 150 W. It was also found that the output voltages were strongly dependent on the position and thickness of the SiO₂ thin films in the ZnO/SiO₂-stacked multilayer devices, in addition to the processing conditions.

2. Materials and Methods

All the ZnO and SiO₂ thin films were deposited using an RF magnetron sputtering technique (Hanback Electronics, Korea). The standard deposition conditions included a base pressure of 2.7×10^{-6} Torr, working pressure of 1.0×10^{-2} Torr, and RF sputtering power of 200 W. Flexible ITO-coated polyethylene naphthalate (PEN) (Hanalin Tech, Gumi-shi, Gyeongsangbuk-Do, Korea) was used as a substrate for the purpose of making wearable devices. All samples were prepared to have the same size of 3 cm × 6 cm.

Various interlayer SiO₂ and ZnO thin films with different thicknesses were deposited at different positions in order to determine which ZnO/SiO₂-stacked multilayer configurations would generate better output voltages. At all stages of the experiments, the ZnO layer for SZS-MGs was deposited for one hour while for ZSZ-MGs, both the upper and lower ZnO layers were deposited respectively for 30 min. Immediately after depositing all the ZnO and SiO₂ film layers, the as-deposited device samples

were annealed in an electric dehydration vacuum furnace (Daesung Electric Furnace, Ansan-City, Gyunggi-Do, Korea) at 150 °C for one hour. Then, the top Ag electrodes were made by coating Ag paste (CANS, ELCOAT P-100, Jinchemical, Korea) onto the annealed devices using the doctor blading technique [18]. Next, aluminum wires were connected to the ITO bottom electrode and to the Ag paste top electrode of each device. Each sample device was evaluated under a mechanical bending/unbending test with a fixed moving speed and interval in a linear motion bending/unbending stage (Labtech Science, Korea), as shown in Figure 1.

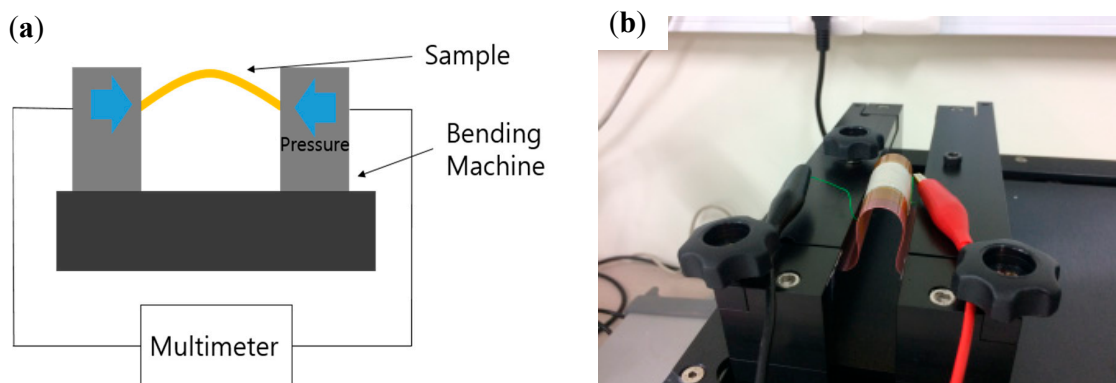


Figure 1. Output voltage measurement system used in this work: (a) schematic diagram and (b) real sample bending/unbending stage.

First of all, to identify which SiO_2 layer positions would generate better output voltages, we investigated two large device groups, i.e., SZS-MGs and ZSZ-MGs, illustrated in Figures 2 and 3, respectively. Moreover, the effects of the working pressure and deposition power on the SiO_2 films were investigated in more detail to understand their influence on the output voltage. Both sputtering targets (ZnO : 4" diameter \times 0.25" thick and SiO_2 : 4" diameter \times 0.125" thick) used for film deposition were manufactured by iTASCO, Korea. The output voltages were measured using a Keysight 34401A (CA, USA) digital multimeter. The piezoelectric micro-energy generators were bent with the middle part raised, also known as forward bending. The output voltages were measured while bending/unbending each device for 300 cycles.

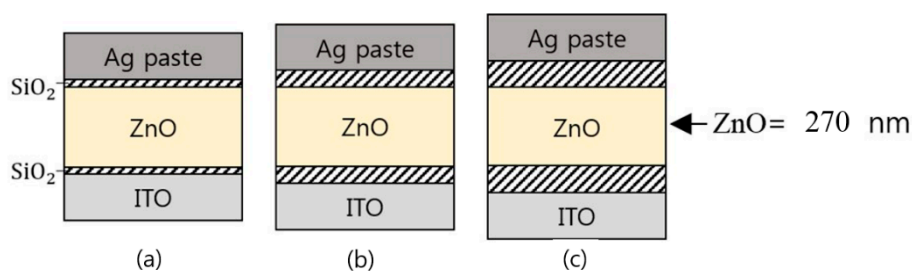


Figure 2. Schematic diagrams of three $\text{SiO}_2/\text{ZnO}/\text{SiO}_2$ micro-energy generators (SZS-MGs) with different SiO_2 thin films. (a) Upper SiO_2 thickness = 78 nm, lower SiO_2 thickness = 40 nm; (b) upper SiO_2 thickness = 90 nm, lower SiO_2 thickness = 63 nm; (c) upper SiO_2 thickness = 146 nm, lower SiO_2 thickness = 110 nm. ITO: indium tin oxide.

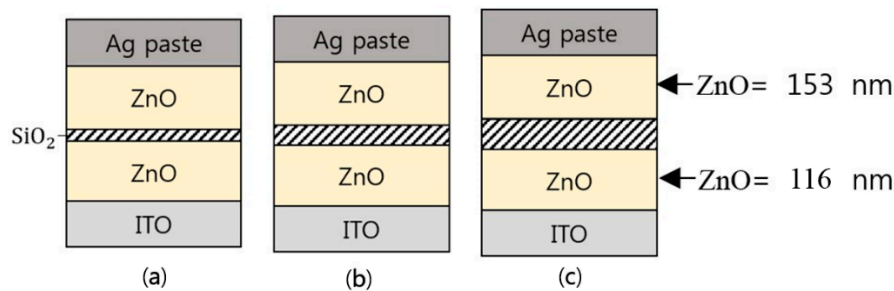


Figure 3. Schematic diagrams of three ZnO/SiO₂/ZnO micro-energy generators (ZSZ-MGs) with different SiO₂ thin films. (a) SiO₂ thickness = 17 nm; (b) SiO₂ thickness = 52 nm; (c) SiO₂ thickness = 141 nm.

3. Results and Discussion

A basic piezoelectric device consisting solely of a single layer of ZnO was fabricated for use as a control (reference) sample, as shown in Figure 4. For comparison, we designed and fabricated various kinds of new piezoelectric micro-energy generator devices by stacking both ZnO and SiO₂ films in an effort to further enhance the output voltage. As shown in Figure 2, the SZS-MGs are composed of a ZnO layer sandwiched between two SiO₂ layers. In contrast, the ZSZ-MGs are composed of a silicon dioxide (SiO₂) layer sandwiched between two ZnO layers, as shown in Figure 3. The ZnO layer for SZS-MGs was deposited for one hour while for ZSZ-MGs, both the upper and lower ZnO layers were deposited respectively for 30 minutes with an RF power of 200 W, resulting in a total thickness of about 270 nm. The SiO₂ layers were deposited by sputtering with an RF power of 200 W for 5, 15, and 30 min, respectively. The output voltages were measured and compared to find out which device configurations could generate higher output voltages.

While the control MG device made up of a single layer of ZnO alone showed a relatively low output voltage of 0.7 mV, as shown in Figure 4, better output voltages were obtained from the ZnO/SiO₂-stacked film devices, i.e., the SZS-MGs and ZSZ-MGs illustrated in Figures 2 and 3. This is considered to be mainly due to the inserted SiO₂ insulating layers. The measured output voltages of the three SZS-MGs illustrated in Figure 2 are plotted in Figure 5. In the case of the devices with SiO₂ films deposited for times in the range from 5 min to 30 min, they produced slightly better output voltages ranging from about 0.9 to 1.7 mV. This seems to suggest that the thicker SiO₂ layers lead to better output voltages, but the magnitude of the output voltage is still small. The measured output voltages of the three ZSZ-MGs shown in Figure 3 are plotted in Figure 6. The ZSZ-MGs showed output voltages about 9 times larger than those of the SZS-MGs. The ZSZ-MG device with a SiO₂ film interlayered between both the top and bottom ZnO layers was observed to generate about 15 mV of peak to peak (P–P) output voltage where the SiO₂ film was deposited for 15 min. The deposition conditions of ZnO and SiO₂ thin films used for the SZS-MGs and ZSZ-MGs, mentioned respectively in Figures 5 and 6, are summarized in more detail in Table 1.

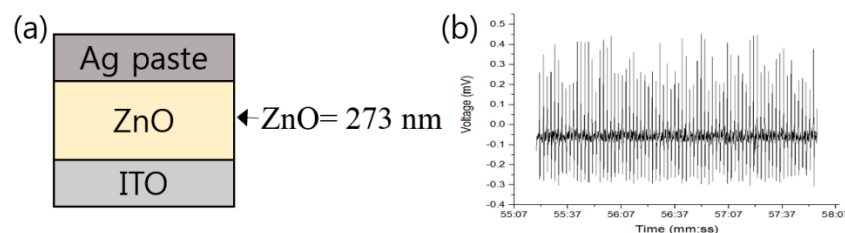


Figure 4. (a) Schematic diagram of control MG with a single ZnO layer used as a reference sample; and (b) its output voltage variation ($V_{p-p} \sim 0.7$ mV) (ZnO film thickness = 273 nm).

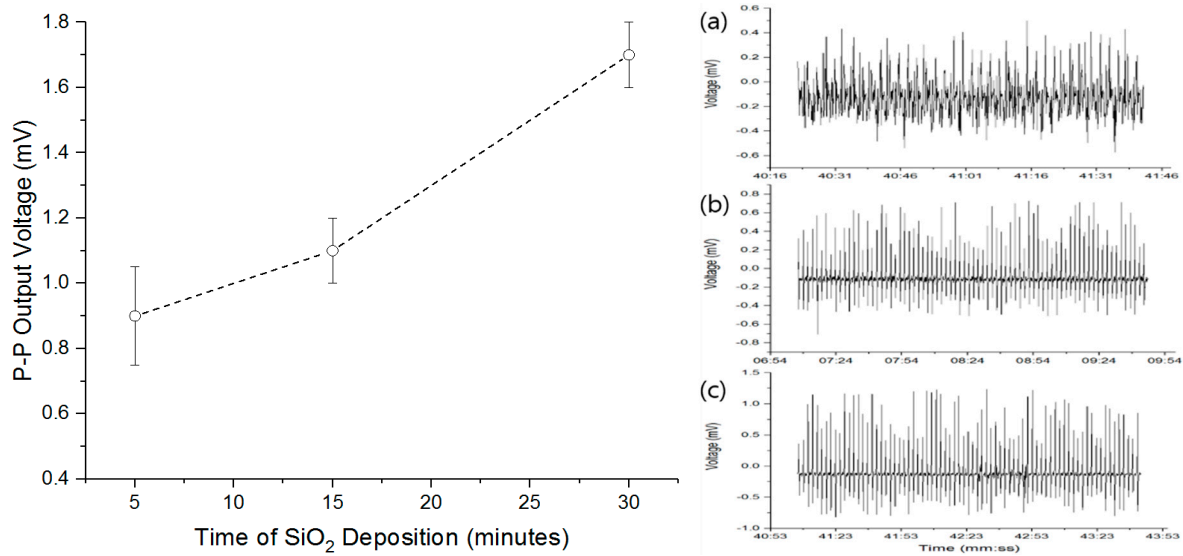


Figure 5. (Left) Peak to peak (P–P) output voltages of three SZS-MGs as a function of the SiO₂ deposition time. (Average deposition rate of SiO₂ = 7.05 nm/min, ZnO = 4.55 nm/min at 200 W deposition power). (Right) Output voltage variations of the SZS-MGs with SiO₂ thin films deposited for (a) 5 min, (b) 15 min, and (c) 30 min, respectively.

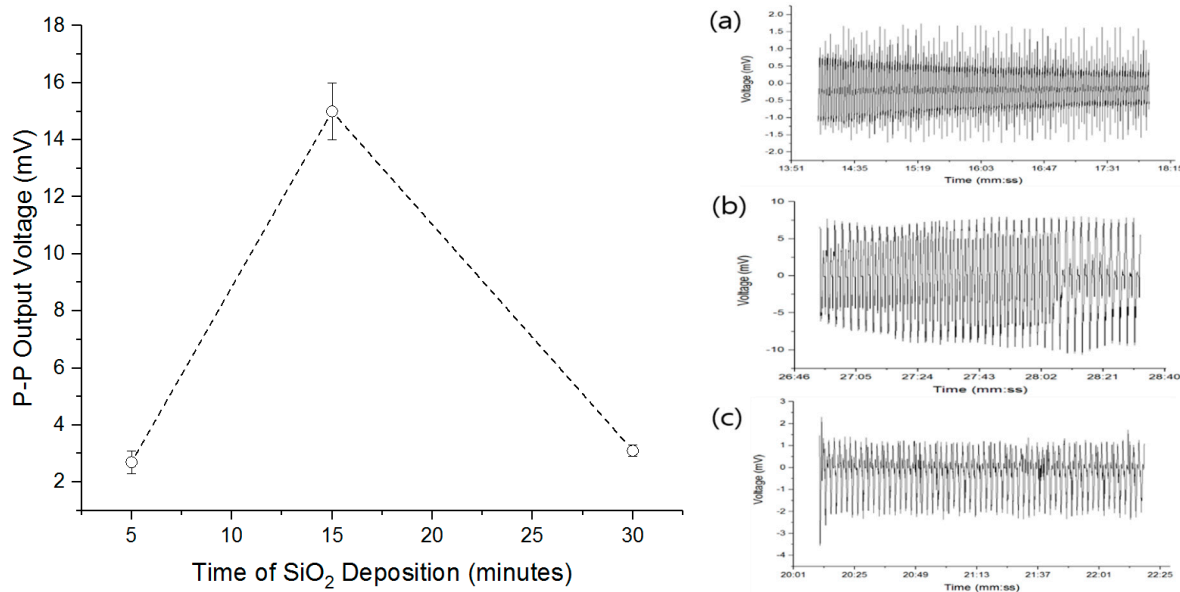


Figure 6. (Left) Peak to peak (P–P) output voltages of three ZSZ-MGs as a function of the SiO₂ deposition time (Average deposition rate of SiO₂ = 3.85 nm/min, ZnO = 4.48 nm/min at 200 W deposition power). (Right) Output voltage variations of three ZSZ-MGs with SiO₂ thin films deposited for (a) 5 min, (b) 15 min, and (c) 30 min, respectively.

Table 1. Deposition conditions of ZnO and SiO₂ thin films for both SiO₂/ZnO/SiO₂ micro-energy generators (SZS-MGs) and ZnO/SiO₂/ZnO micro-energy generators (ZSZ-MGs) shown in Figures 5 and 6, respectively.

Film	ZnO	SiO ₂
Power (W)	200	200
Pressure (Torr)	1.0×10^{-2}	1.0×10^{-2}
Gas Flow (sccm)	N ₂ O (12) + Ar (18)	Ar (20)
Substrate Temperature (°C)	29	29
Target-Substrate Distance (cm)	12	12
Deposition Time (min)	SZS-MG: 60 ZSZ-MG: 30 (upper layer)/ 30 (lower layer)	5, 15, 30

Therefore, the ZSZ-MGs showed better output voltages than the SZS-MGs after 300 bending/unbending cycles. Additionally, among the ZSZ-MGs, the SiO₂ films deposited at 200 W for 15 min were of a desirable thickness, leading to the generation of the highest output voltages. This is believed to be due to the blockage of electrons. The two thicker SiO₂ layers surrounding the ZnO layer, as shown in Figure 2, can make it harder for electrons to flow into and out of the ZnO layer. This would suppress the screening effect while forming potential barriers, leading eventually to the elevation of the output voltage. On the other hand, when the SiO₂ film is placed as an interlayer between the top and bottom ZnO layers, as shown in Figure 3, there will be a critical or optimum thickness of the SiO₂ film layer which acts as a barrier that helps to elevate the output voltage while suppressing the screening effect. Moreover, a thinner SiO₂ layer may allow relatively more electrons to flow through the oxide film. If the SiO₂ layer is thicker than the critical or optimum thickness, it may more effectively block the flowing of the electrons generated by the piezoelectric effect, thus reducing the net output voltage. The more detailed descriptions on the precise physical/electrical mechanism of our multilayered thin film devices remain our future work.

Table 2 shows the thicknesses of individual film layers. The SiO₂ film thickness was about 52 nm when the top ZnO film was 153 nm thick and the bottom one was 116 nm thick. Figure 7 shows a cross-sectional view of the SiO₂ layer sandwiched between the top and bottom ZnO layers. The inset in the figure shows a high-resolution transmission electron microscopy (HRTEM) image and selected area electron diffraction (SAED) pattern of the ZnO film, indicating that the ZnO film has a crystalline form [15]. The distance between the (0002) planes was found to be 0.26 nm. This observation is meaningful because the crystallinity of the ZnO film can have an influence on its ionic polarization, eventually affecting its piezoelectricity.

Comparing the output voltages of the SZS and ZSZ devices shown in Figures 5 and 6, the ZSZ devices were found to exhibit better performance than the SZS devices. From this observation, we were inspired to further investigate the ZSZ devices in the hope of enhancing the device performance even further. First, we investigated the effects of working pressure on the output voltages of the ZSZ devices. We fabricated five ZSZ-MG samples with SiO₂ films deposited under various working pressures of 5×10^{-1} , 1×10^{-1} , 5×10^{-2} , 1×10^{-2} , and 5.1×10^{-3} Torr. Figure 8 shows the variations in the peak to peak (P-P) output voltages of these ZSZ-MGs with SiO₂ thin films deposited under different working pressures, indicating that there is a strong dependence of the output voltage on the working pressure during SiO₂ film deposition. Table 3 summarizes the deposition conditions of both the ZnO and SiO₂ thin films used to fabricate these ZSZ-MGs. As shown in Figure 8, the ZSZ device with an SiO₂ film deposited for 15 min with an RF power of 200 W at working pressure of 5×10^{-2} Torr produced the best output performance ($V_{P-P} = 4.5$ mV) among the five samples. As shown in Figure 9, the surface and grain morphologies of the deposited SiO₂ films seem to be affected by the working pressure, which may eventually have an influence on the output voltage.

The SiO₂ surface morphology appears to vary considerably depending on the working pressure. The scanning electron microscope (SEM) images in Figure 9 show that the SiO₂ grains became smaller and denser as the working pressure was decreased.

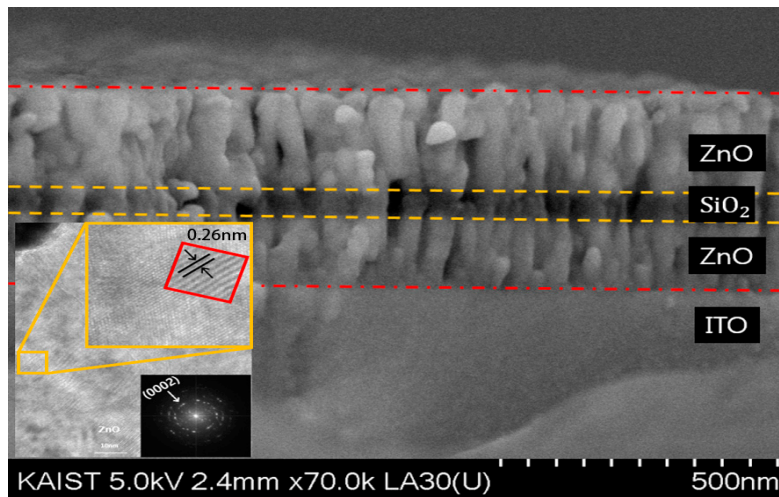


Figure 7. Cross-sectional scanning electron microscope (SEM) image of a typical ZSZ-MG sample fabricated in this work. The inset shows a high-resolution transmission electron microscope (HRTEM) image of the ZnO film along with its selected area electron diffraction (SAED) pattern.

Table 2. Average thickness of each film layer in ZSZ-MGs in Figure 6.

Time of SiO ₂ thin film deposition (min)	5	15	30
Thickness of SiO ₂ thin film (nm)	17	52	141
Thickness of the upper ZnO thin film (nm)		153	
Thickness of the lower ZnO thin film (nm)		116	

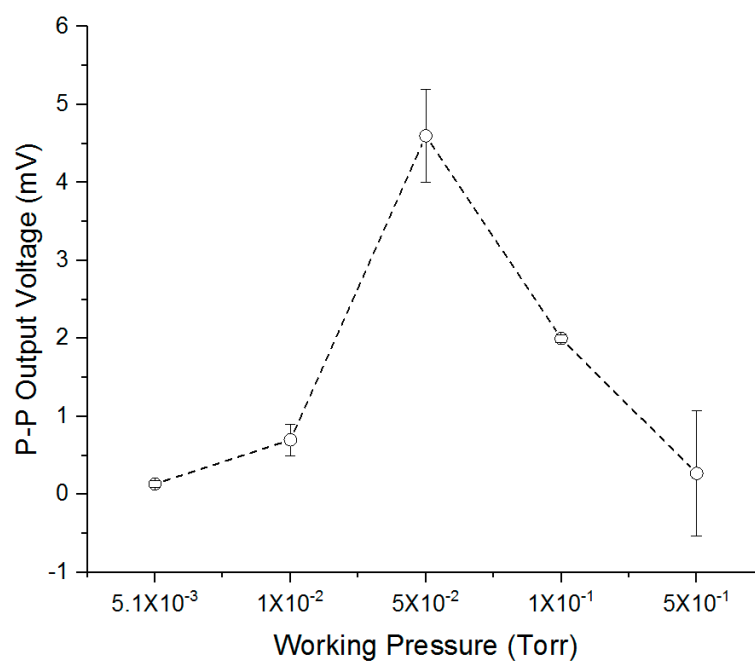


Figure 8. Peak to peak (P-P) output voltage variations of various ZSZ-MGs with different SiO₂ thin films deposited under different working pressures. Deposition power is fixed at 200 W.

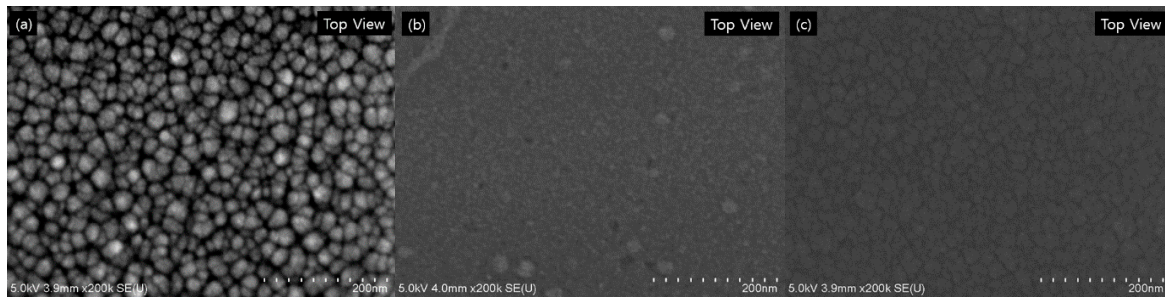


Figure 9. SEM images obtained at 200 k times magnification showing the surface morphologies of the SiO₂ thin films deposited under three different working pressures: (a) 5.0×10^{-1} , (b) 5.0×10^{-2} , and (c) 5.0×10^{-3} Torr. Deposition power was fixed at 200 W.

Table 3. Deposition conditions of both ZnO and SiO₂ thin films used to fabricate the ZSZ-MGs in Figure 8.

Film	ZnO	SiO ₂
Power (W)	200	200
Pressure (Torr)	1.0×10^{-2}	5.0×10^{-1} , 1.0×10^{-1} , 5.0×10^{-2} , 1.0×10^{-2} , 5.0×10^{-3}
Gas Flow (sccm)	N ₂ O (12) + Ar (18)	Ar (20)
Substrate Temperature (°C)	29	29
Target-Substrate Distance (cm)	12	12
Deposition Time (min)	30 (upper layer)/30 (lower layer)	15
Film Thickness (nm)	271	50, 54, 57, 51, 59

Second, we also investigated the effects of deposition power on the output voltage of the ZSZ-MG devices. We fabricated four different ZSZ-MG devices with SiO₂ films deposited using various deposition powers of 50, 100, 150, and 200 W. The output voltage variations of those ZSZ-MGs are plotted in Figure 10. To maintain a similar thickness for each deposited oxide film, the deposition time alone was controlled to be inversely proportional to the applied RF power while keeping all other process conditions constant.

The device measurements showed that the largest output voltage (35 mV) was generated by the ZSZ-MG device with a silicon dioxide (SiO₂) thin film deposited using 150 W for 22.5 min, as shown in Figure 10. This may be due to the formation at 150 W of the relatively fine-grained surface morphology shown in Figure 11. The deposition conditions of both ZnO and SiO₂ thin films are summarized in Table 4.

Table 4. Deposition conditions of both ZnO and SiO₂ thin films used to fabricate the ZSZ-MGs in Figure 10.

Film	ZnO	SiO ₂
Power (W)	200	50, 100, 150, 200
Pressure (Torr)	1.0×10^{-2}	1.0×10^{-2}
Gas flow (sccm)	N ₂ O (12) + Ar (18)	Ar (20)
Substrate temperature (°C)	29	29
Target-substrate distance (cm)	12	12
Deposition time (min)	30 (upper layer)/30 (lower layer)	45, 30, 22.5, 15

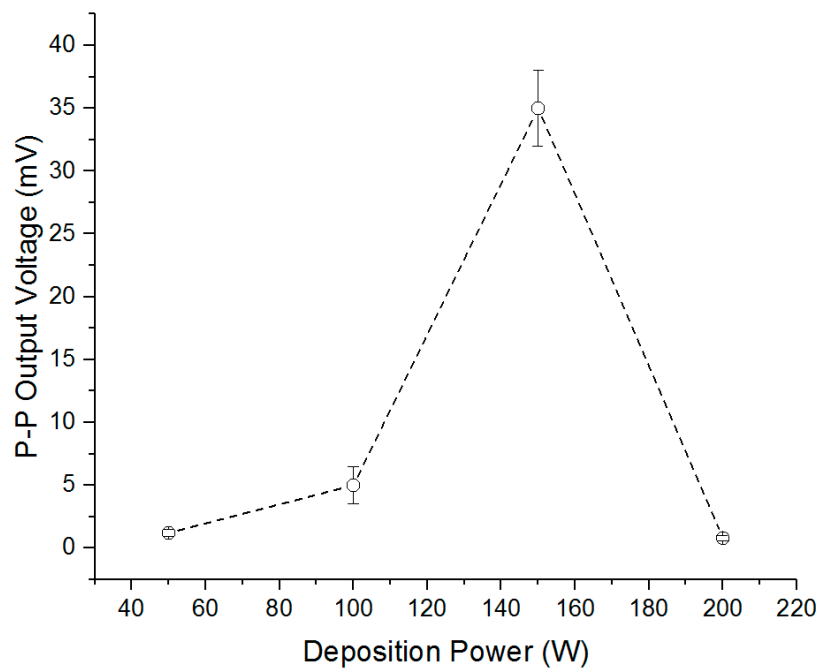


Figure 10. Peak to peak (P-P) output voltage variations of the ZSZ-MGs with SiO₂ thin films deposited at various radio frequency (RF) powers. Deposition working pressure was fixed at 1.0×10^{-2} Torr.

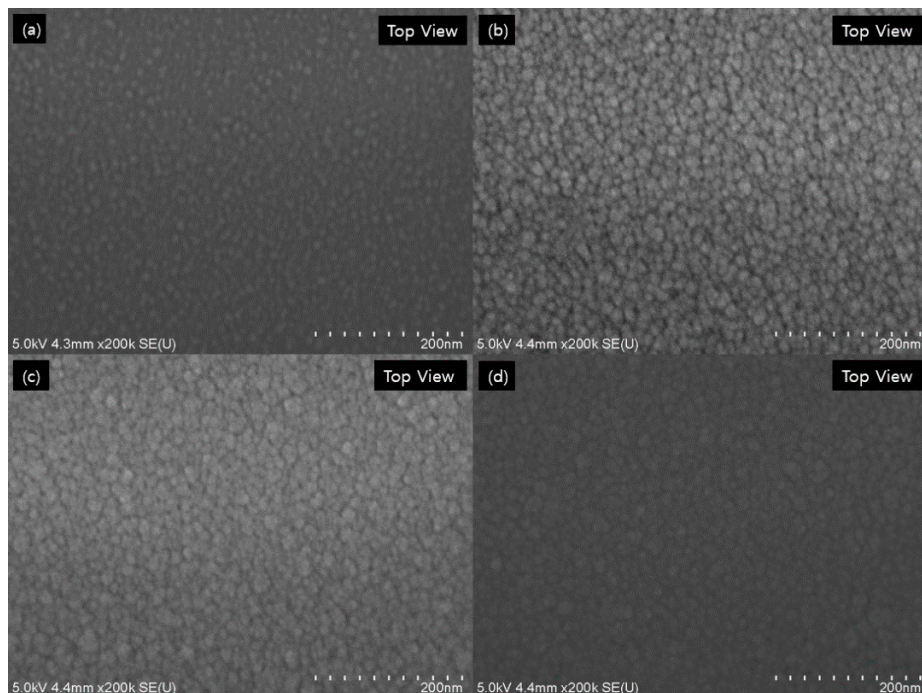


Figure 11. SEM images obtained at 200 k times magnification showing SiO₂ thin films deposited using various RF powers: (a) 50 W, (b) 100 W, (c) 150 W, and (d) 200 W.

4. Conclusions

Various ZnO/SiO₂-stacked thin film structures were studied for flexible micro-energy harvesting devices. Two types of micro-energy generators, ZSZ-MGs and SZS-MGs, were fabricated by stacking both SiO₂ and ZnO thin films on top of each other using an RF magnetron sputtering technique, all on flexible ITO-coated PEN substrates. The resulting devices were then characterized. In particular,

the effects of SiO₂ film thickness and position on device performance were investigated in terms of the output voltage in comparison to a ZnO single-layer micro-energy generator used as a control device. Compared to the ZnO single-layer control device, the ZSZ-MGs showed much better output voltages while the SZS-MGs showed only slightly better output voltages. The output voltages of the ZSZ-MGs depended strongly on the working pressure during deposition of the SiO₂ thin films. The highest peak to peak (P–P) output voltage was about 35 mV obtained from the ZSZ-MG device where the SiO₂ thin film was deposited at an RF power of 150 W. In the ZSZ or SZS devices with ZnO/SiO₂-stacked thin film structures, the output voltages were found to be significantly affected by the position and thickness of the SiO₂ film layer(s) with respect to the ZnO layer(s) in addition to their processing conditions. This work could be usefully applied to the development of more advanced energy harvesting devices based on ZnO/SiO₂-stacked multilayer structures.

Author Contributions: Conceptualization, Investigation, Data Curation, Writing-Original Draft Preparation, Visualization, Y.C.; Equipment and Materials Managing and Preparation, J.B. Writing-Review and Editing, Supervision, Y.G.

Funding: This research was funded by Ministry of Education, grant number [2016R1D1A1B01007074].

Acknowledgments: This research was supported by Basic Science Research Program through the National Research Foundation of Korea (NRF) funded by the Ministry of Education (Grant No. 2016R1D1A1B01007074).

Conflicts of Interest: The authors declare no conflict of interest.

References

1. Chen, J.; Wang, Z.L. Reviving Vibration Energy Harvesting and Self-Powered Sensing by a Triboelectric Nanogenerator. *Joule* **2017**, *1*, 480–521. [[CrossRef](#)]
2. Wang, X.; Song, J.; Liu, J.; Wang, Z.L. Direct-Current Nanogenerator Driven by Ultrasonic Waves. *Science* **2007**, *316*, 102–105. [[CrossRef](#)] [[PubMed](#)]
3. Yang, W.; Chen, J.; Zhu, G.; Yang, J.; Bai, P.; Su, Y.; Jing, Q.; Cao, X.; Wang, Z.L. Harvesting Energy from the Natural Vibration of Human Walking. *ACS Nano* **2013**, *7*, 11317–11324. [[CrossRef](#)] [[PubMed](#)]
4. Chen, J.; Yang, J.; Li, Z.; Fan, X.; Zi, Y.; Jing, Q.; Guo, H.; Wen, Z.; Pradel, K.C.; Niu, S.; et al. Networks of Triboelectric Nanogenerators for Harvesting Water Wave Energy: A Potential Approach toward Blue Energy. *ACS Nano* **2015**, *9*, 3324–3331. [[CrossRef](#)] [[PubMed](#)]
5. Zhang, L.; Zhang, B.; Chen, J.; Jin, L.; Deng, W.; Tang, J.; Zhang, H.; Pan, H.; Zhu, M.; Yang, W.; et al. Lawn Structured Triboelectric Nanogenerators for Scavenging Sweeping Wind Energy on Rooftops. *Adv. Mater.* **2015**, *28*, 1650–1656. [[CrossRef](#)] [[PubMed](#)]
6. Zhang, N.; Chen, J.; Huang, Y.; Guo, W.; Yang, J.; Du, J.; Fan, X.; Tao, C. A Wearable All-Solid Photovoltaic Textile. *Adv. Mater.* **2015**, *201528*, 263–269. [[CrossRef](#)] [[PubMed](#)]
7. Zi, Y.; Lin, L.; Wang, J.; Wang, S.; Chen, J.; Fan, X.; Yang, P.; Yi, F.; Wang, Z.L. Triboelectric-Pyroelectric-Piezoelectric Hybrid Cell for High-Efficiency Energy-Harvesting and Self-Powered Sensing. *Adv. Mater.* **2015**, *27*, 2340. [[CrossRef](#)] [[PubMed](#)]
8. Olutade, B.L.; Hunt, W.D. Sensitivity Analysis of a Thin Film Bulk Acoustic Resonator Ladder Filter. In Proceedings of the International Frequency Control Symposium, Orlando, FL, USA, 30 May 1997. 5828130.
9. Jeong, C.K.; Baek, C.; Kingon, A.I.; Park, K.I.; Kim, S.H. Lead-Free Perovskite Nanowire-Employed Piezopolymer for Highly Efficient Flexible Nanocomposite Energy Harvester. *Small* **2018**, *14*. [[CrossRef](#)] [[PubMed](#)]
10. Demartin Maeder, M.; Damjanovic, D.; Setter, N. Lead Free Piezoelectric Materials. *J. Electroceram.* **2004**, *13*, 385–392. [[CrossRef](#)]
11. Hinchet, R.; Lee, S.; Ardila, G.; Monte's, L.; Mouis, M.; Wang, Z.L. Design and Guideline Rules for the Performance Improvement of Vertically Integrated Nanogenerator. *J. Ener. Pow. Eng.* **2013**, *7*, 1816.
12. Yang, R.; Qin, Y.; Dai, L.; Wang, Z.L. Power Generation with Laterally Packaged Piezoelectric Fine Wires. *Nat. Nanotechnol.* **2008**, *4*, 34–39. [[CrossRef](#)] [[PubMed](#)]
13. Lee, M.; Chen, C.; Wang, S.; Cha, S.; Park, Y.; Kim, J.; Chou, L.; Wang, Z.L. A Hybrid Piezoelectric Structure for Wearable Nanogenerators. *Adv. Mater.* **2012**, *24*, 1759–1764. [[CrossRef](#)] [[PubMed](#)]

14. Lee, E.; Park, J.; Yim, M.; Kim, Y.; Yoon, G. Characteristics of Piezoelectric ZnO/AlN-Stacked Flexible Nanogenerators for Energy Harvesting Applications. *Appl. Phys. Lett.* **2015**, *106*, 023901. [[CrossRef](#)]
15. Lee, E.; Park, J.; Yim, M.; Jeong, S.; Yoon, G. High-Efficiency Micro-Energy Generation Based on Free-Carrier-Modulated ZnO: N Piezoelectric Thin Films. *Appl. Phys. Lett.* **2014**, *104*, 213908. [[CrossRef](#)]
16. Yin, B.; Qiu, Y.; Zhang, H.; Lei, J.; Chang, Y.; Ji, J.; Luo, Y.; Zhao, Y.; Hu, L. Piezoelectric Performance Enhancement of ZnO Flexible Nanogenerator by a NiO-ZnO p-n Junction Formation. *Nano Energy* **2015**, *14*, 95–101. [[CrossRef](#)]
17. Park, H.; Lee, K.Y.; Seo, J.; Jeong, J.; Kim, H.; Choi, D.; Kim, S. Charge-Generating Mode Control in High-Performance Transparent Flexible Piezoelectric Nanogenerators. *Adv. Funct. Mater.* **2011**, *21*, 1187–1193. [[CrossRef](#)]
18. Lee, K.Y.; Kumar, B.; Seo, J.; Kim, K.; Sohn, J.I.; Cha, S.N.; Choi, D.; Wang, Z.L.; Kim, S. P-Type Polymer-Hybridized High-Performance Piezoelectric Nanogenerators. *Nano Lett.* **2012**, *12*, 1959–1964. [[CrossRef](#)] [[PubMed](#)]
19. Przędziecka, E.; Chusnutdinow, S.; Guziewicz, E.; Snigurenko, D.; Stachowicz, M.; Kopalko, K.; Reszka, A.; Kozanecki, A. The p-ZnO:N/i-Al₂O₃/n-GaN Heterostructure-Electron Beam Induced Profiling, Electrical Properties and UV Detectivity. *J. Phys. D Appl. Phys.* **2015**, *48*, 325105. [[CrossRef](#)]
20. Lei, J.; Yin, B.; Qiu, Y.; Zhang, H.; Chang, Y.; Luo, Y.; Zhao, Y.; Ji, J.; Hu, L. Flexible Piezoelectric Nanogenerator Based on Cu₂O-ZnO p-n Junction for Energy Harvesting. *RSC Adv.* **2015**, *5*, 59458–59462. [[CrossRef](#)]
21. Lim, Y.S.; Seo, S.G.; Kim, B.B.; Choi, H.; Seo, W.; Cho, Y.S.; Park, H. Effects of SiO₂ Interlayer on Electrical Properties of Al-Doped ZnO Films under Bending Stress. *Electron. Mater. Lett.* **2012**, *8*, 375–379. [[CrossRef](#)]



© 2018 by the authors. Licensee MDPI, Basel, Switzerland. This article is an open access article distributed under the terms and conditions of the Creative Commons Attribution (CC BY) license (<http://creativecommons.org/licenses/by/4.0/>).